Periodicals of Engineering and Natural Sciences ISSN 2303-4521
Vol. 9, No. 2, June 2021, pp.1124-1140

Flexural behavior of two-layer beams made with normal and lightweight concrete layers

Hayder Kadhem Adai AL-Farttoosi[1], Haleem K. Hussain[2], Oday A. Abdulrazzaq[3]
[1] Civil Engineering, University of Basrah
[2] Civil Engineering, University of Basrah
[3] Civil Engineering, University of Basrah

ABSTRACT

In this paper, twelve concrete beams with two different layers of concrete were evaluated as a simply supported beam under four-points loading. The beams assembled of two different types of concrete layers, one of which was normal-weight concrete (NWC) and the other was lightweight aggregate concrete (LWAC). The investigated parameters were the thickness of the lightweight concrete to the overall depth of beams (hLW/h), and the compressive strength of normal and lightweight concrete. Due to the weak lightweight aggregates used, lightweight aggregate concrete exhibits more brittleness and lower stiffness. Therefore, the viability of compensating for this degradation and providing a layer of normal concrete seems to be very interesting in such beams. The behavior of beams was evaluated based on cracking, failure mode, flexural strength, maximum deflection, stiffness, and toughness. The results showed slight variations on the majority of the above-mentioned performance aspects of two-layer beams compared to fully normal concrete beams. While there were great enhancements compared to fully LWAC beams. The variants were mainly attributable to the efficacy of using LWAC in providing lower stiffness and lower tensile strength. The experimental results have been compared to predicted values using the ACI 318-19, with some modifications for the equations to be matched with two-layer beams, the comparison was in terms of the deflection due to service load, moment capacity, and cracking moment.

Keywords: Layered beams, two-layer RC beams, LWAC beams, NWC beams.

Corresponding Author:

Hayder Kadhem Adai AL-Farttoosi,
Civil Engineering,
University of Basrah,
Iraq/ Basra.
E-mail: Hayder.k.alfarttoosi@gmail.com

1. Introduction

The rapid development of high-rise buildings, larger sizes and longer spans concrete structures necessitated the use of concrete that performed well in terms of strength, toughness, and light weight, the latter being related to the density of concrete. A lower density leads to a reduction in dead loads in structural design and foundations, which allows for a decrease with in horizontal inertia actions on buildings in earthquake regions. In comparison to normal weight concrete (NWC), lightweight concrete (LWC) shows more brittleness and lower stiffness[1], [2].

These variance in mechanical properties of NWC and LWC reveals an idea to combined both concretes in structural composite elements [3], [4]. The structural composite elements are typically made up of two materials: one carries the majority of the flexural loads, and the other is a thick, while the low-weight core increases shear ability and the section's moment of inertia. Such types of composite system are becoming more commonly adopted in the peculiarly industry of conservative infrastructure construction, due to their cost-effectiveness, high strength to weight ratio, excellent durability, good impact resistance, excellent fatigue and corrosion resistance, and design flexibility. Such composite systems are mainly used for structural roofs, walls, floors, and bridge decks. [5].

Over the previous few years, considerable research has been conducted on the action of beams composed of two layers with two different materials. However, despite its incredible potential, its use in developing sustainable composite beams remains limited. lately, some researches on a full-scale two-layer beam and a continuous two-layer beam were performed, which consisted of normal strength concrete in the tensile zone and high strength concrete with steel fiber in the compression zone [6], [7]. Other researchers have been focused on replacing the tension zone with Engineered Cementitious Composite (ECC) to improve the tensile strength of the concrete around the main steel reinforcement [8]–[10]. Mohsin et al. [11] introduced analyses of a new two-layer RC beam, where the compression zone and tension zone were made of high strength concrete and normal strength concrete, respectively. Dybel and Wałach [12] investigated the bond strength development between two concrete layers in an experimental study. The types of normal concrete (NC) to high-performance concrete (HPC) and HPC to HPC, as well as comparisons with NC-to-NC specimens, have been established.
The essential objectives of this study is to evaluate the strength and behavior of two-layer beams consisting of normal and lightweight concrete, the parameters have been chosen to investigate the effect of combining these two materials together in the same two-layer beams. The depth of each layer and compressive strength of normal and lightweight concrete were the main parameters of this study.

2. Experimental program

As shown in Fig. 1 and Fig. 2a twelve two-layer reinforced concrete beams were prepared and tested as simply supported beams under a four-point loading schematic. All the beams having similar cross-section of 140 × 200 mm and total length is 1700 mm. The considered parameters in this research are the thickness of lightweight aggregate concrete layer and the compressive strength of lightweight aggregate concrete in compression and/or tension zones while the compressive strength of normal concrete in compression zone only. The Beams were divided into four groups the first group based on ratio of thickness of LWAC layer to overall depth of the beam h_{LW}/h: 0%, 25%, 50%, 75%, and 100% where the LWAC in the tension zone (TZ). The second and third groups investigate the effect of compressive strength of NWC AND LWAC in the compression zone (CZ), while the last group investigates the compressive strength of LWAC in the TZ.

3. Preparation of beams

The prepared lightweight aggregate concrete mixtures are considered to be structural LWAC mixtures with an equilibrium density of 1801,1953 and 2031 kg/m^3, where it meets ASTM C330 and ACI 318-19 for structural LWAC classifications. The mixture components include: ordinary Portland cement Type I, pumice as lightweight aggregate with a maximal particle size of 25 mm and 1.75 of dry specific gravity, normal weight fine aggregate with 2.65 of specific gravity. The absorptions of the lightweight coarse and normal weight fine aggregates were 10% and 1.1%, respectively. The normal concrete mixtures are made with normal coarse aggregate of a maximal particle size of 19 mm and dry specific gravity of 2.66. Table 1 listing the used mixes proportions for six mixtures. A barrel mixer with 0.20 m^3 of capacity have been used for concrete mixing with 0.10 m^3 as a batch volume, which appropriate to cast two beams and six cylinders with100 mm diameter and 200 mm height.
Smooth wood molds were used to cast the beams. The wood molds have been marked with grooves to specify the level of concrete layers as shown in the Fig. 2b. Prior to pouring the concrete, the steel reinforcements were placed in the wood molds then positioned with adequate cover. The beams were cast into two layers, each of which was properly compacted with an electrical vibrator. After 72 hours, the beams were removed out of molds and wrapped with wet blankets and plastic sheets for 28 days of curing. The compressive strength, splitting tensile strengths, and the modulus of elasticity of the tested cylinders after 28 days summarizes in Table 1. deformed steel bars with f_y = 620 MPa were used for the longitudinal steel and stirrups. As top reinforcement, two bars with a diameter of 10 mm were used, and two bars of with diameter of 16 mm were used as bottom reinforcement. 10 mm in diameter stirrups were used with 50 mm spacing distributed in shear spans to avoid the shear failure. The top, bottom, and side concrete cover were 33 mm to the center of bars as shown in Fig. 1. The designation of beams included a combination of letters and numbers: For example, (B1N-1L25) B stands for flexural beams, Part 1N is the first normal concrete mix ID ,1L for first lightweight aggregate concrete mix ID and 25 indicate the ratio of lightweight layer thickness to overall depth of beams.

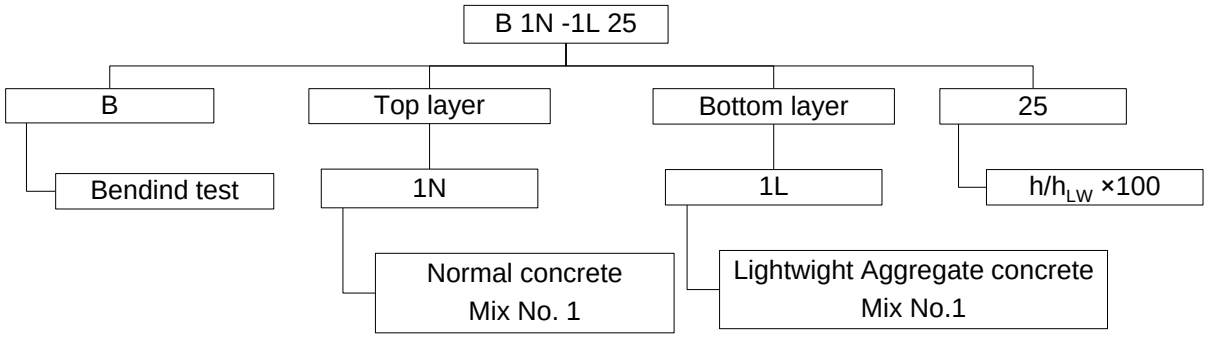

Table 1. Properties of material and mixes proportions (kg/m^3)

ID	water	Cement	Sand	Aggregate		SF	SP	w_c (kg/m^3)	f'_c MPa	f_{ct} MPa	E_c MPa
				NWA	LWA						
1N	150	401	682	1007	-	35	4.80	2432	49.3	4.46	36534
2N	185	420	718	1077	-	0	2.10	2412	33.1	3.12	31139
3N	200	400	720	1054	-	0	0.00	2396	25.5	2.45	29194
1L	226	300	520	-	633	23	0	1801	23.2	2.50	13952
2L	200	450	562	-	473	50	3.95	1953	28.5	2.20	14590
3L	226	510	880	-	371	55	4.46	2031	35.1	2.05	17295

where SF: silica fume, SP: Super-plasticizer, w_c: equilibrium density, NWA: Normal Wight Aggregate, LWA: Lightweight Aggregate.

Grade 75, (620 MPa) reinforcement steel have been used. All the reinforcing bars met the requirements of ASTM A615. Fig. 3 shows the stress-strain curve of steel reinforcement bars. Table 2 summarizes the specifications of tested beams.

Table 2. Beams' specifications

Beam	Layer thickness of		h_{LW}/h	Type of concrete	
	NWC (mm)	LWAC (mm)		Top layer	Bottom layer
B1N	-	-	0%	NWC	-
B1N-1L25	150	50	25%	NWC	LWAC
B1N-1L50	100	100	50%	NWC	LWAC
B1N-1L75	50	150	75%	NWC	LWAC
B1L	-	-	100%	-	LWAC
B1L-1N50	100	100	50%	LWAC	NWAC
B2L-1N50	100	100	50%	LWAC	NWAC
B3L-1N50	100	100	50%	LWAC	NWAC
B1N-2L50	100	100	50%	NWC	LWAC
B1N-3L50	100	100	50%	NWC	LWAC
B2N-1L50	100	100	50%	NWC	LWAC

4. Testing setup

As shown in Fig. 4, the experimental tests were performed as a simply supported beams with 1400 mm clear span under four-point loading, distance between the two loading points was 300 mm. Two steel supports and steel bearing plates with cross-section of 20 mm × 100 mm were constructed in order to withstand the applied load without any deformation that could have an effect on the results. A universal hydraulic testing machine

with a portable load cell of a capacity of 470 kN has been used for load application under 50 N/s loading rate. One LVDT was placed vertically at the center of the beam to measure the mid-span deflection. A computerized data logger system was used to collect and analyze the experimental data.

Three strain gauges have been used for strain measurement in the reinforcement and concrete. One of strain gauges was installed on the lower part of the main longitudinal reinforcement at mid-span, while the other two strain gauges were installed on concrete surface at 25 mm and 75 mm of beam depth. Fig. 1 shows the locations of the strain gauges and LVDT. During the test, any cracks that formed on the surface of the beam were marked and measured using a digital crack width meter at load increments, both the deflections and strains have been monitored till the beam failure.

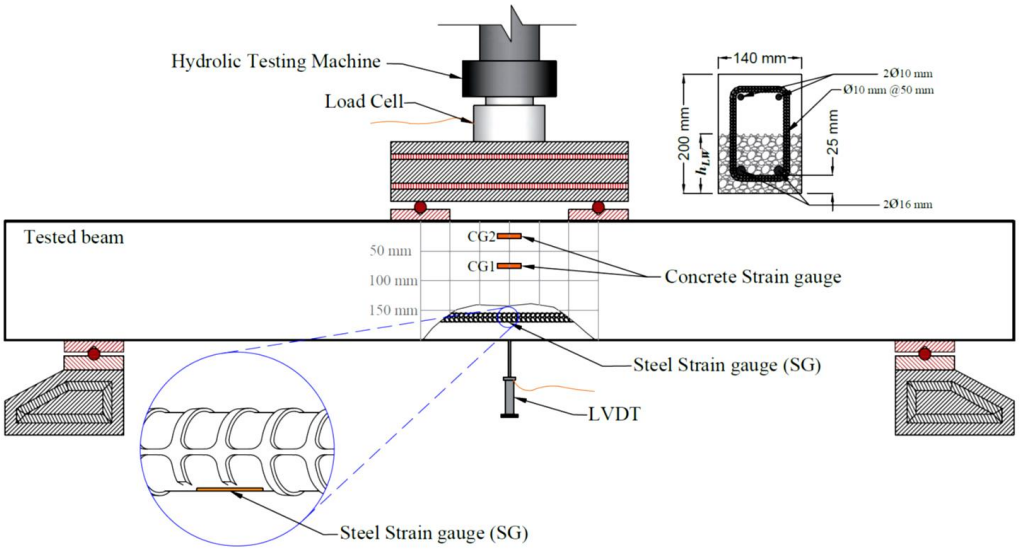

Figure 1. Four points loading set up configuration

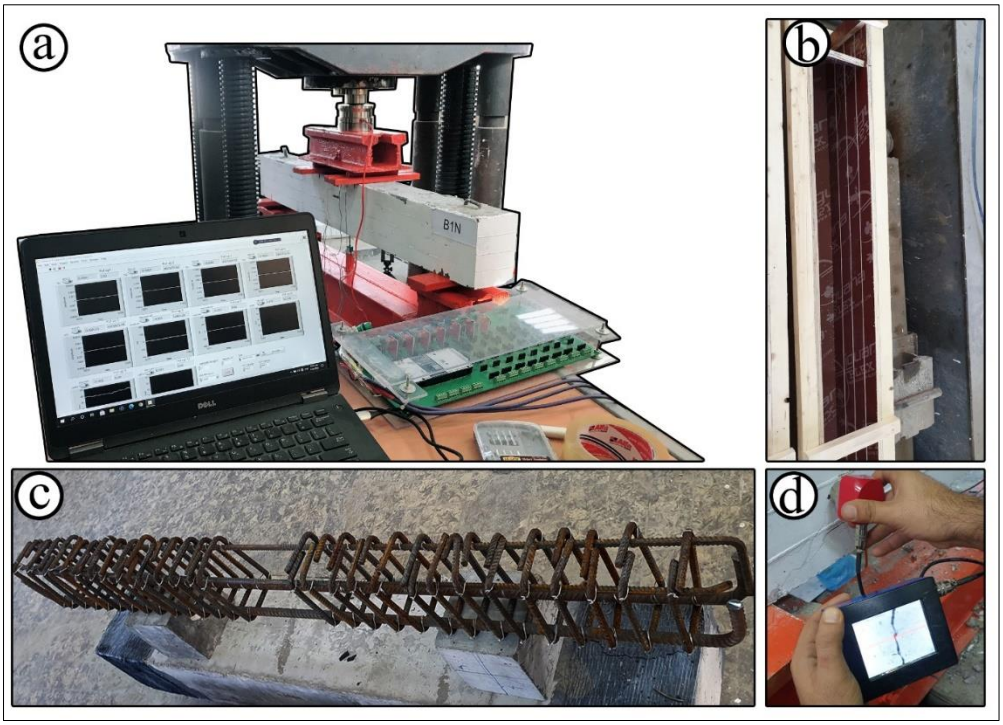

Figure 2. (a) Experimental set up, (b) wood molds, (c) steel reinforcement, and (d) digital crack width meter.

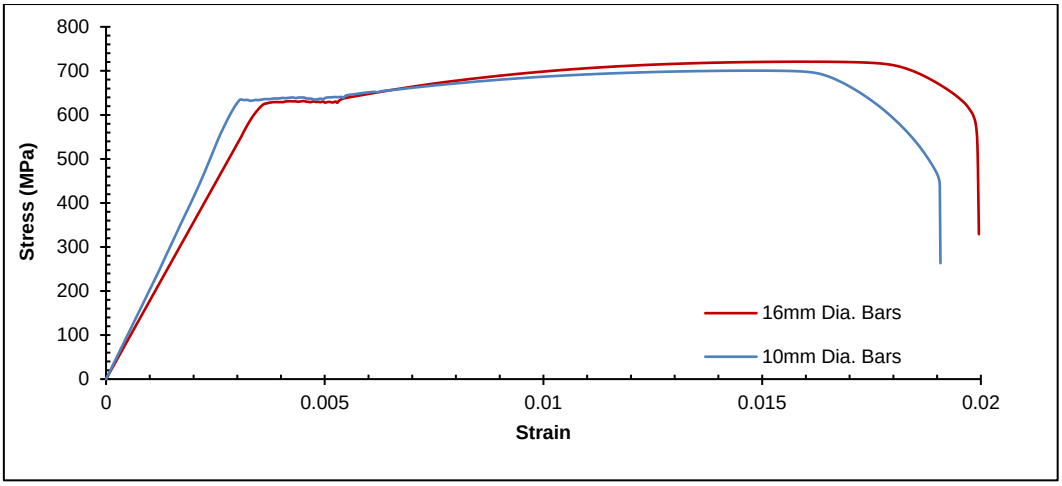

Figure 3. Stress-strain curve of reinforcement bars.

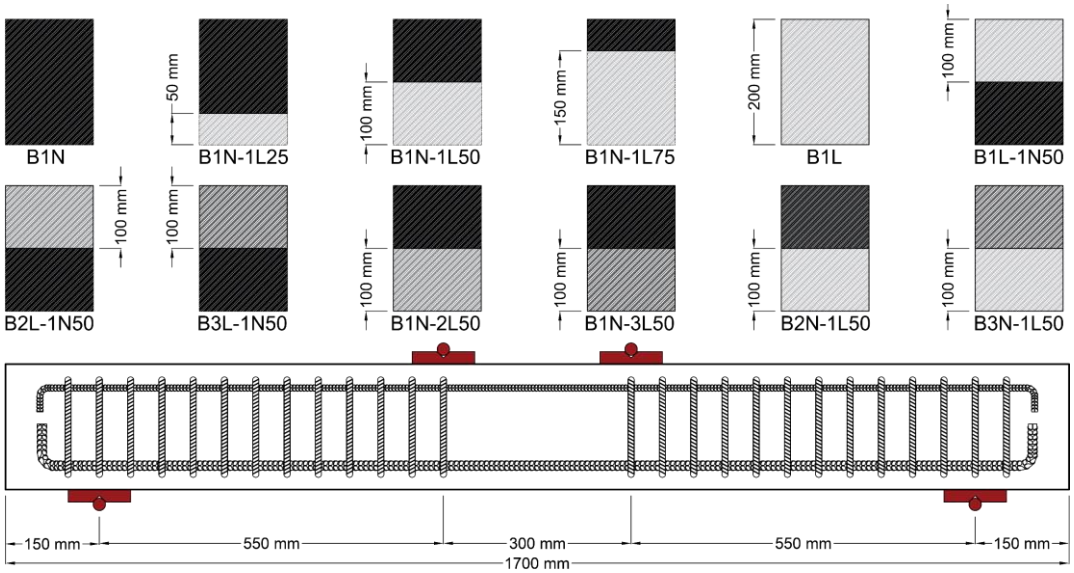

Figure 4. Beams' layout and reinforcement distribution.

5. Results and discussions

5.1. Cracking and failure modes

In terms of crack propagation, the behavior of the both control and two-layer beams were similar except for crack spacing, compared to the cracks of control beam, the cracks of the two-layer beams were closer to each other. All of the beams in failed the flexure. The longitudinal tension steel yielded first in all of the beams, followed by concrete crushing at constant moment zone, which is a ductile failure mode, generally known as tension failure. Fig. 5 shows the patterns of cracks generated during the testing of the beams. In tested beams, the first appearance of cracks in the center of the beam where the bending moment is constant, followed by formation of the additional flexural cracks. As shown in the Table 3, the first crack loads for all beams are ranged between 8.7 kN and 12.06 kN, as well as the ratio of ultimate load to first crack load (P_u/P_{cr}) was between 6.7 to 8.9. In this region, as the loading increased, all cracks propagated almost vertically upward.. Also, as the loading increased, inclined cracks formed and propagated upward on both sides of the constant moment zone. The patterns of cracks were comparable; slightly consistent distribution as the lightweight aggregate concrete layer increases. Furthermore, the number, length, and distribution of cracks increase as h_{LW}/h increased. Decreasing the NWC compressive strength in the compressive zone decreases the number of cracks with significant concrete crushing in the compressive zone. The pattern of cracks did not significantly change with increasing the LWAC compressive strength on the compressive or tension layers.

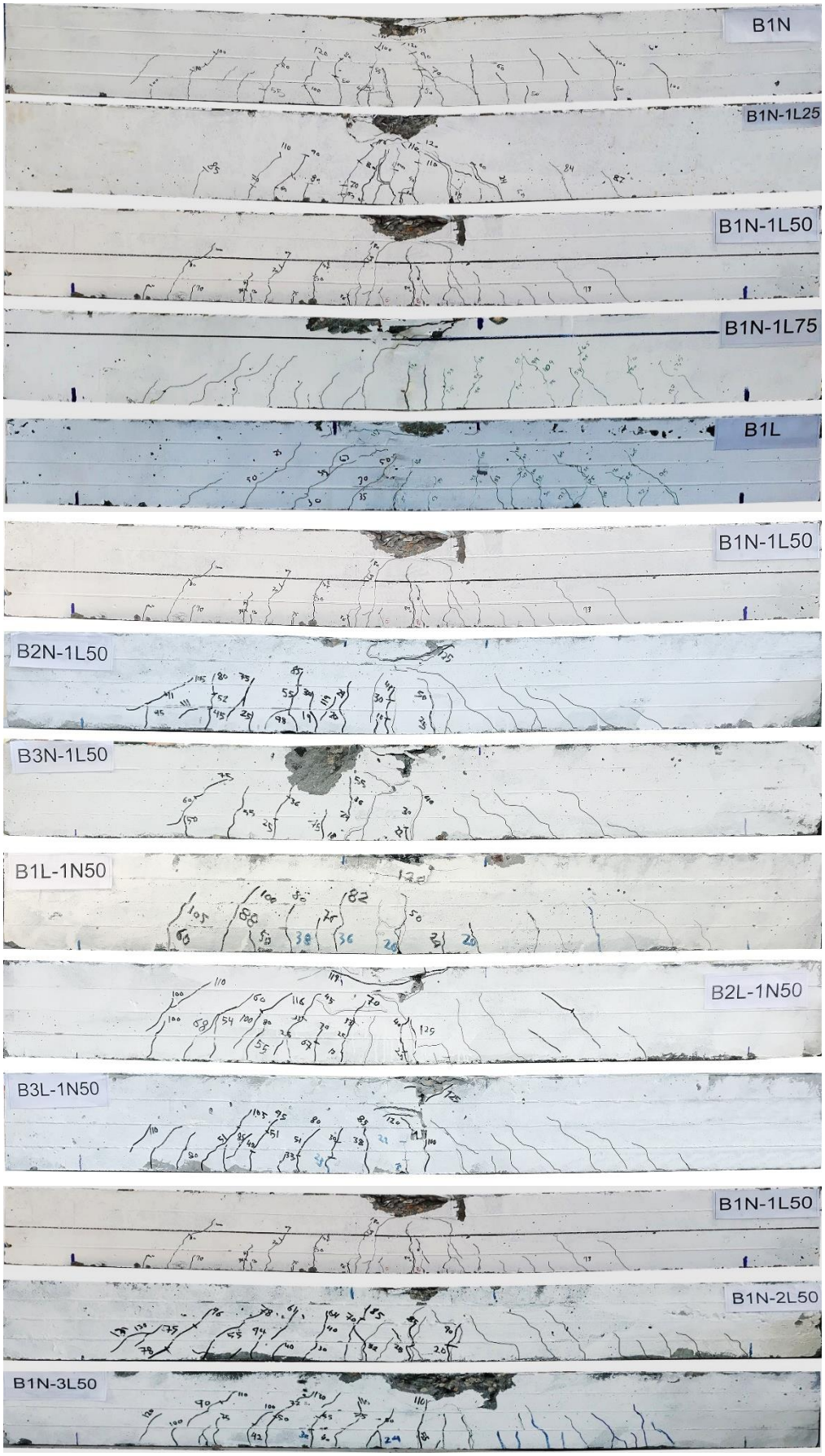

Figure 5. Crack pattern of tested beams

5.2. Load-deflection curves

Load-deflection curves for all beams are shown in Fig. 6. These curves are depicted in a way that enables comparison of the effect of layer thickness in the same group of beams, as well as the influence of compressive strength of NWC and LWAC. Clearly, the ultimate strength, and also the ultimate deflection, both decrease as the h_{LW}/h increases. The load-deflection curves tend to indicate how the beams behaved as the load increased up to failure, with such a pre-cracking segment that is almost a straight line. Slope of the curve changes after cracking, indicating a reduction in beam stiffness before the yielding of tension steel reinforcement. After yielding, the beams' strength increased slightly, followed by an approximately flat top segment with a small reduction in strength. even though the existence of a lightweight aggregate concrete layer increased ultimate deflection, the behavior of beams remained ductile, with the exception of fully lightweight aggregate concrete beams and concrete layer at the compression zone with compressive strength 23.2 MPa, where the load-deflection curve deteriorated after ultimate load.

The influence of compressive strength of concrete on the ultimate load and cracking was typical, both of which increased as compressive strength increased. Nevertheless, it is also interesting to realize that the maximum deflection incurred by the beams with $\rho = 1.72\%$ (which exceeds ρ'_{max}) smaller, and the corresponding ductility is as low as the companion beams with higher ρ'_{max}. Also, it is important to mention that steel reinforcements limits of the beams with LWAC were designed mainly based on testing NWC beams. Furthermore, this could be due to the small spacing of the stirrups, which provides powerful confinement to the concrete.

Table 3 summarizes the key behavior characteristics of all the tested beams. The ultimate load on each beam was normalized to the control beam in its group, and the results are presented Fig. 7 as a bar chart graph. The results show that the effectiveness of the two-layer composite beams. Increasing depth ratio (h_{LW}/h) from 0% (full NWC beam) to 25% and 50%, there was no significant change in the ultimate strength the decreasing was 0.13% and 0.44% respectively, after that for 75% depth ratio there was a 3.4% decrease in the ultimate strength of the composite beams. For beam with 100% depth ratio (full LWAC beam), the decreasing in the ultimate strength was 8.65%. Decreasing the compressive strength of NWC in the compression zone from 49.3 to 33.1 and 25.5 MPa, there was a significant decreasing in ultimate strength of the two-layer beams to 5.24% and 8.91% respectively. While increasing the compressive strength of LWAC in the tension zone there were no significant improvements in the ultimate strength. Increasing the compressive strength of the LWAC in the compression zone from 23.2 to 28.5 and 35.1 MPa increases the ultimate strength of the composite beams by 4.94% and 7.79% respectively. While increasing the LWAC compressive strength in the tension zone from 23.2 to 28.5 and 35.1 MPa decreases the ultimate strength of two beams by 0.05% and 1.02% respectively. Fig. 7 shows the ultimate load and final deflection of each beam normalized with respect to the control beam for each group.

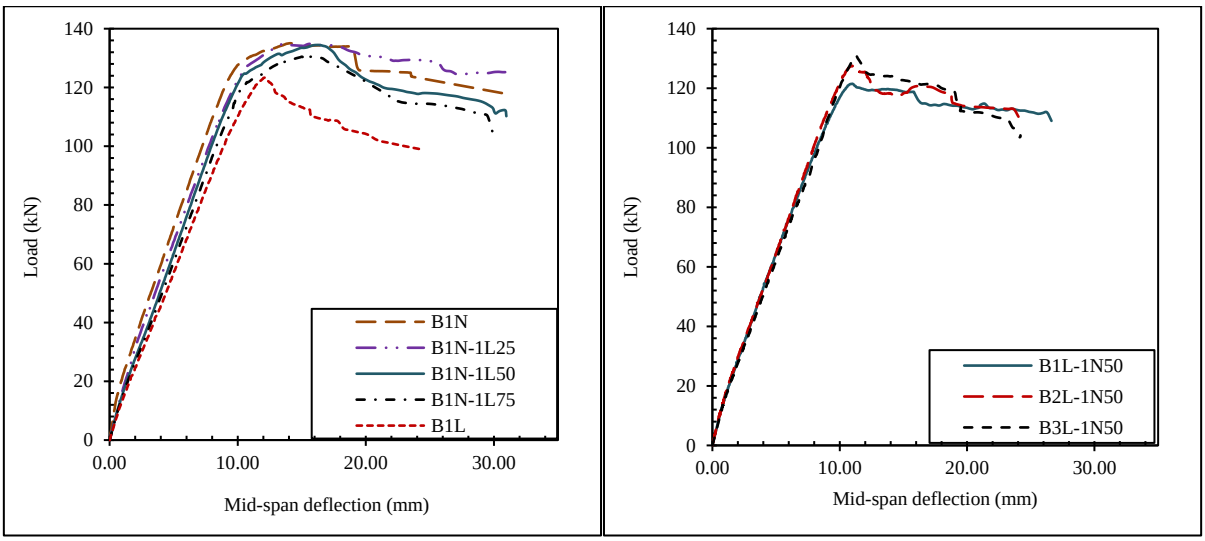

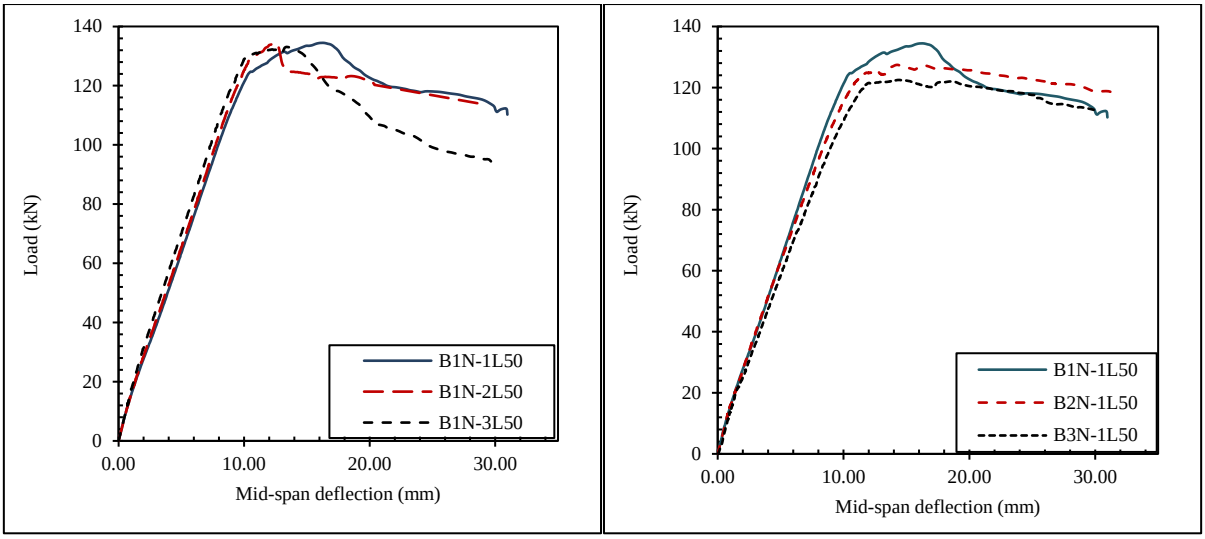

Figure 6. Load-deflection curves.

Table 3. Test results of tested beams

Beam ID	P_u (kN)	δ_u (mm)	P_y (kN)	δ_y (mm)	P_{cr} (kN)	P_{cr}/P_u (%)
B1N	135.05	31.12	99.72	7.21	12.06	8.9
B1N-1L25	134.86	30.88	99.63	7.77	10.87	8.1
B1N-1L50	134.46	30.97	100.93	8.19	8.88	6.6
B1N-1L75	130.45	29.88	98.73	8.33	8.70	6.7
B1L	123.36	24.22	99.32	8.82	8.88	7.2
B2N-1L50	121.49	31.44	102.30	8.56	9.63	7.6
B3N-1L50	127.49	29.98	100.37	8.92	10.21	8.3
B1L-1N50	130.96	26.62	99.36	8.12	10.18	8.4
B2L-1N50	134.46	24.09	100.62	8.00	10.87	8.5
B3L-1N50	134.38	24.19	99.71	8.31	10.95	8.4
B1N-2L50	133.09	28.96	99.14	7.65	8.88	6.6
B1N-3L50	134.46	29.91	102.44	7.61	10.04	7.5

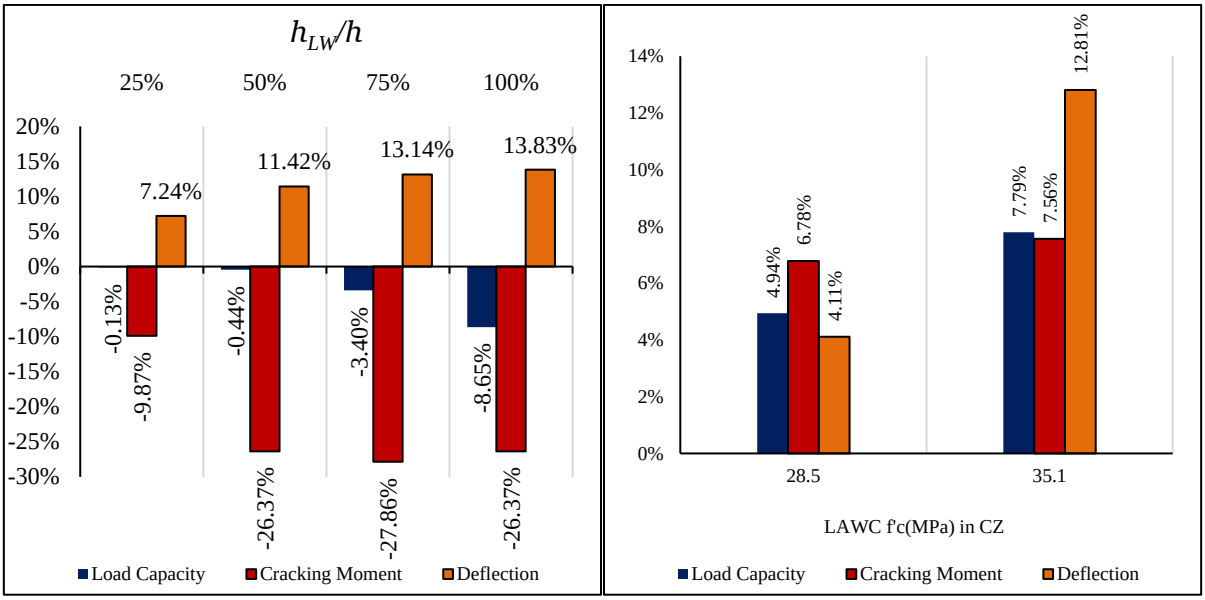

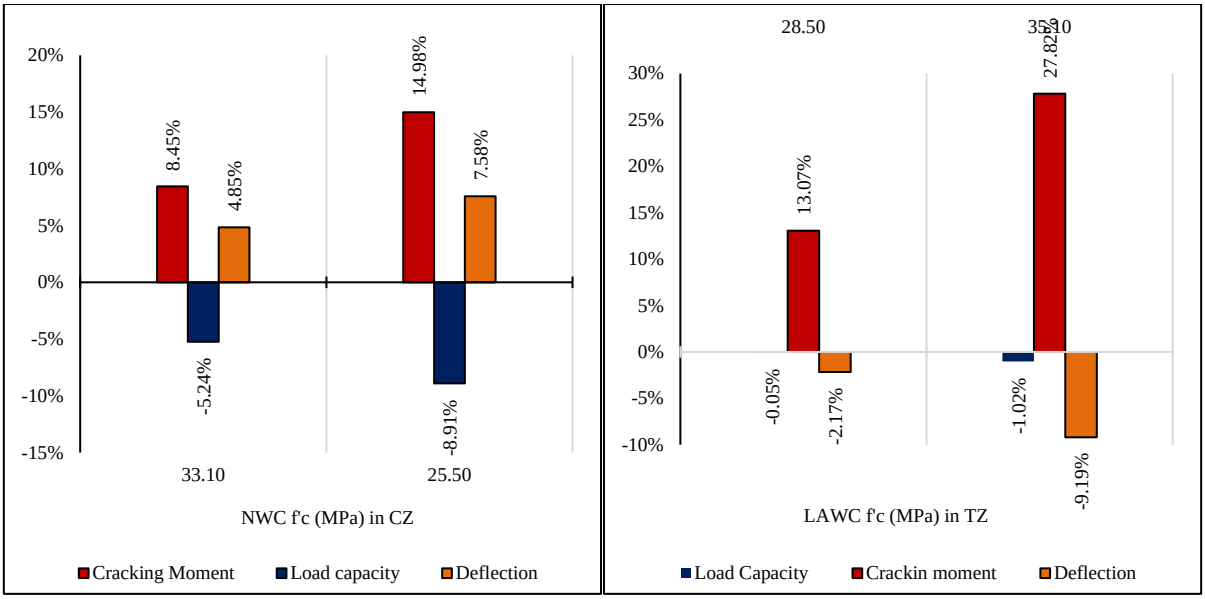

Figure 7. Normalized results vs investigated parameters

5.3. Strain results

Fig. 8 displays the collected concrete strain (CG) corresponding to the load at two points through the depth as shown in Fig. 1. the steel gauge (SG) placed at the bottom of tension steel reinforcement, while the concrete gauges (CG1 and CG2) placed at 25 mm and 75 mm from the top fiber of the beams respectively. At an ultimate stage, the strain readings of concrete may not be accurate due to the rapid development of cracks. The measured concrete strain variants among beams were due to the differences in the concrete type and concrete compressive strength. Tensile strain in the bottom steel reinforcement increased almost linearly up to 70%–80% of the ultimate load, after which point it increased rapidly.

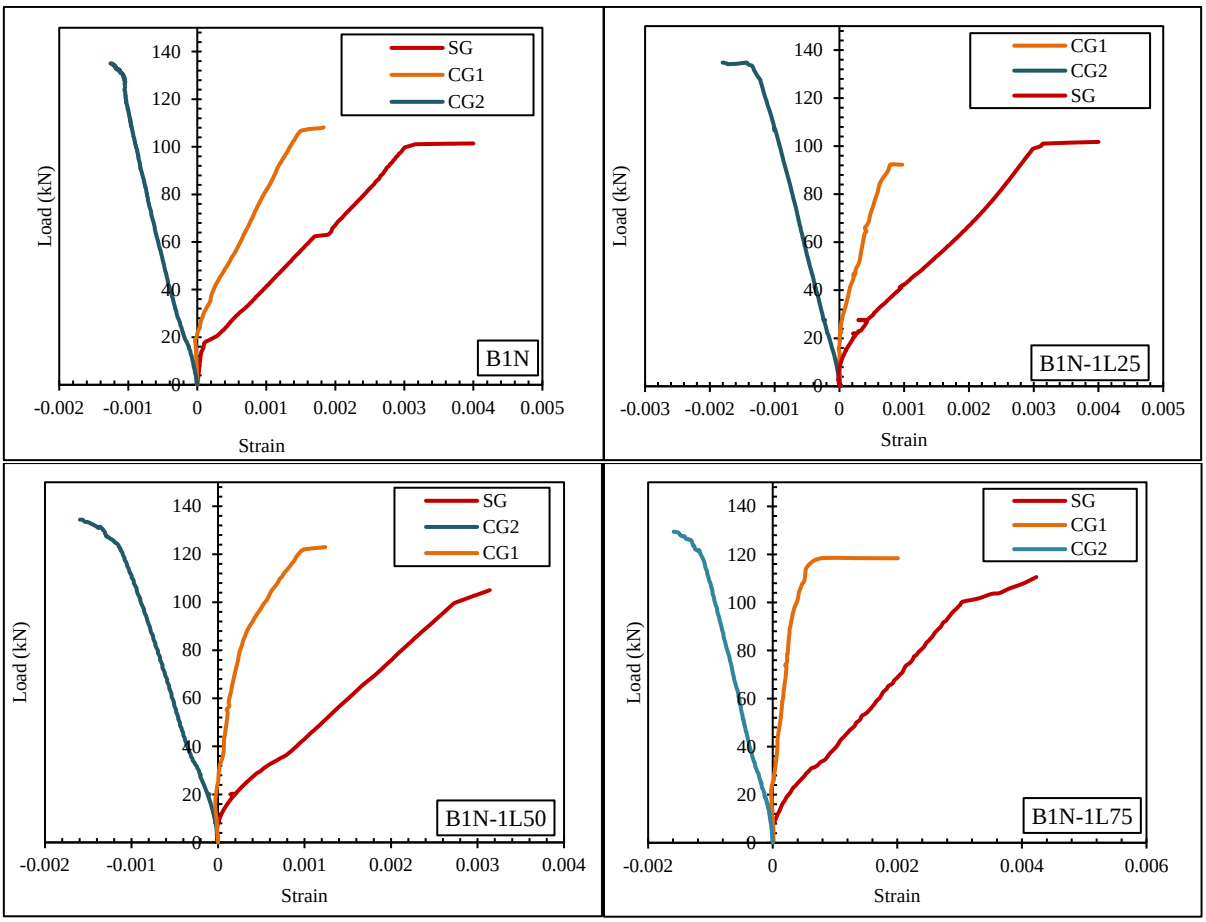

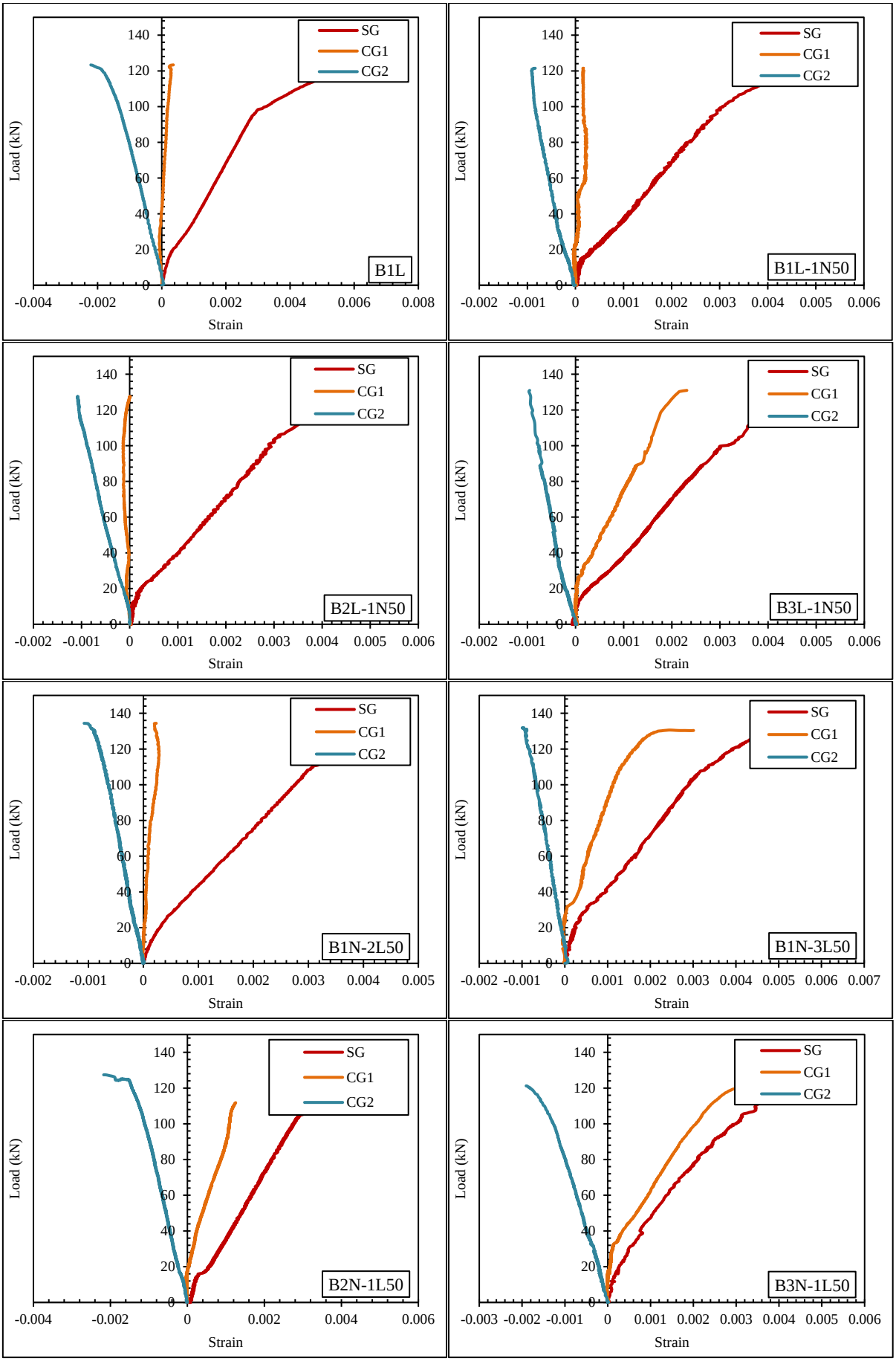

Figure 8. Load-strain curves

5.4. Stiffness

Table 4 summarizes the stiffness characteristics determined for each beam based on the curves illustrated between experimental load and mid-span deflection. The slope of the linear portion of the load-deflection curve before the creation of the first flexural crack is referred to as initial stiffness. On the upward segment of the load-deflection curve, service stiffness is described as the slope of the points corresponding to 50% and 80% of the ultimate load capacity on the load-deflection curve [13]. The stiffness results of each two-layer beam were normalized with respect to the control beam in its group to be compared, and the results are shown in Fig. 9. For the first group the results reveal that the two-layer beams have no significant changes to each other the initial stiffness, while it is with average value about 40% in compared to beam with full NWC and increased about 46% in compare to beams with full LWAC. While the average decrease in service stiffness was 4.47% in compared with B1N and the average increase was 6.68% in compared to B1L. Decreasing the compressive strength of NWC in compression zone from 49.3 to 33.1 and 25.5 MPa decreases the initial and service stiffness by 3.85%-17.74% and 8.5%-10.73% respectively. Increasing the compressive strength of lightweight aggregate concrete in compression zone from 23.2 to 28.5 and 35.1 MPa increases the initial stiffness by 3.87% and 4.96%, and decreases the service stiffness by 9% and 2.39% respectively. Increasing the compressive strength of lightweight aggregate concrete in tension zone from 23.2 to 28.5 and 35.1 MPa increases the initial stiffness by 0.28% and 1.21% while decreases the service stiffness by 6.20% and 6.16% respectively. In all beams, the influence of LWAC layer was significant in values of initial stiffness, conversely of service stiffness.

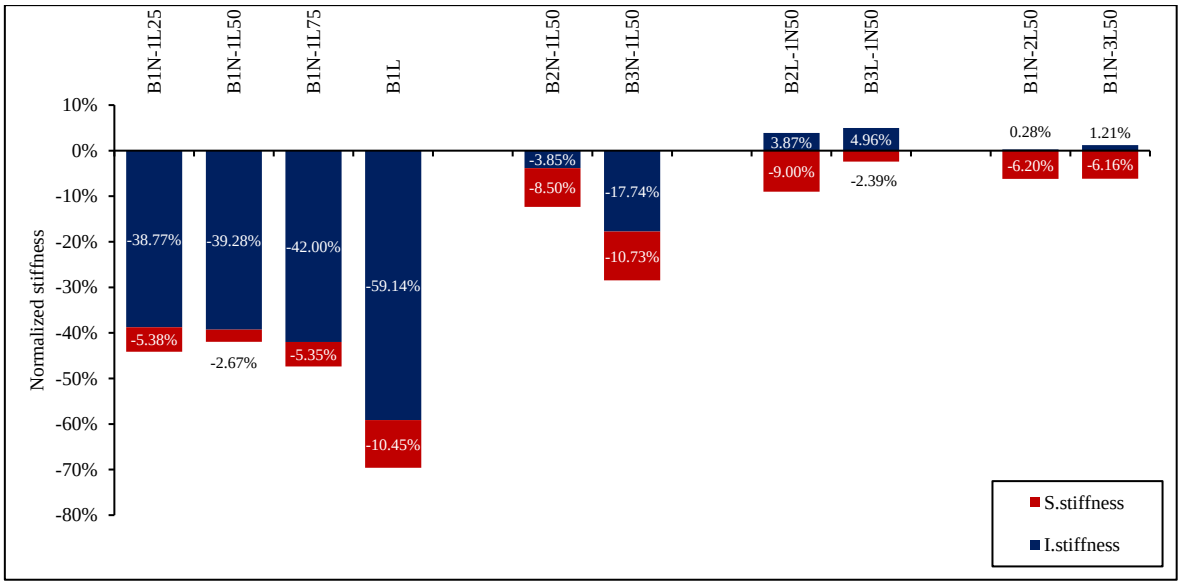

Figure 9. Normalized initial and service stiffness

5.5. Displacement ductility and flexural toughness

Table 3 shows the determined displacement ductility index and flexural toughness values of all beams. Ductility is a highly eligible structural property that indicates the structural member's capability to withstand substantial deflections before failure. The ratio of the ultimate deflection to the first yield deflection can be used to calculate the ductility index values, while the flexural toughness values reflect the total area under the load-deflection curve. The displacement ductility results distinctly show that ductility decreases as h/h_{LW} increases, as shown in Fig. 10, which is expected. However, cautious inspection of Fig. 10 uncovers an important observation in which, for two layer beams the ductility reduced 8.02%, 12.41%, and 16.98% as h_{LW}/h increased from zero to 25%, 50%, and 75% compared to B1N, and increased 44.67%, 37.76%, and 30.58% compared to B1L respectively. Decreasing the compressive strength of NWC in compression zone from 49.3 to 33.1 and 25.5 Mpa the ductility decreased by 2.90% and 11.19% respectively. Increasing the compressive strength of lightweight aggregate concrete in compression zone from 23.2 to 28.5 and 35.1 Mpa the ductility decreased by 8.21% and 11.24% respectively. The displacement ductility increased by 0.09% and 3.96% as the compressive strength of LWAC in tension zone increased from 23.2 to 28.5 and 35.1 MPa.

Toughness results for all beams are shown Fig. 11. The experimental result shows that the flexural toughness decreased for all beams compared to the control beams in the same group which indicates that the effect of the

two layers on toughness is major. The toughness decreased 0.72%, 5.30%, and 11.61% as hLW/h increased from zero to 25%, 50%, and 75% compared to B1N, and increased 58.75%, 51.44%, and 41.35% compared to B1L respectively. Decreasing the compressive strength of NWC in compression zone from 49.3 to 33.1 and 25.5 Mpa the toughness decreased by 3.36% and 8.46% respectively. Increasing the compressive strength of lightweight aggregate concrete in compression zone from 23.2 to 28.5 and 35.1 Mpa the toughness decreased by 9.58% and 9.75% respectively. The toughness decreased by 7.96% and 8.70% as the compressive strength of LWAC in tension zone increased from 23.2 to 28.5 and 35.1 MPa.

Table 4. results of stiffness, displacement ductility and toughness for tested beams

Beam	Initial stiffness (kN/mm)	Service stiffness (kN/mm)	Ductility (mm/mm)	Toughness (kN.mm)
B1N	27.78	12.34	4.32	3398.04
B1N-1L25	17.01	11.68	3.97	3373.51
B1N-1L50	16.87	12.01	3.78	3218.04
B1N-1L75	16.11	11.68	3.59	3003.67
B1L	11.35	11.05	2.75	2125.02
B2N-1L50	16.87	10.99	3.67	3109.89
B3N-1L50	16.22	10.72	3.36	2945.83
B1L-1N50	16.60	11.21	3.28	2552.52
B2L-1N50	17.24	12.21	3.01	2307.95
B3L-1N50	17.43	11.47	2.91	2303.71
B1N-2L50	16.91	12.76	3.79	2961.91
B1N-3L50	17.07	12.75	3.93	2937.93
B1N	27.78	12.34	4.32	3398.04
B1N-1L25	17.01	11.68	3.97	3373.51
B1N-1L50	16.87	12.01	3.78	3218.04

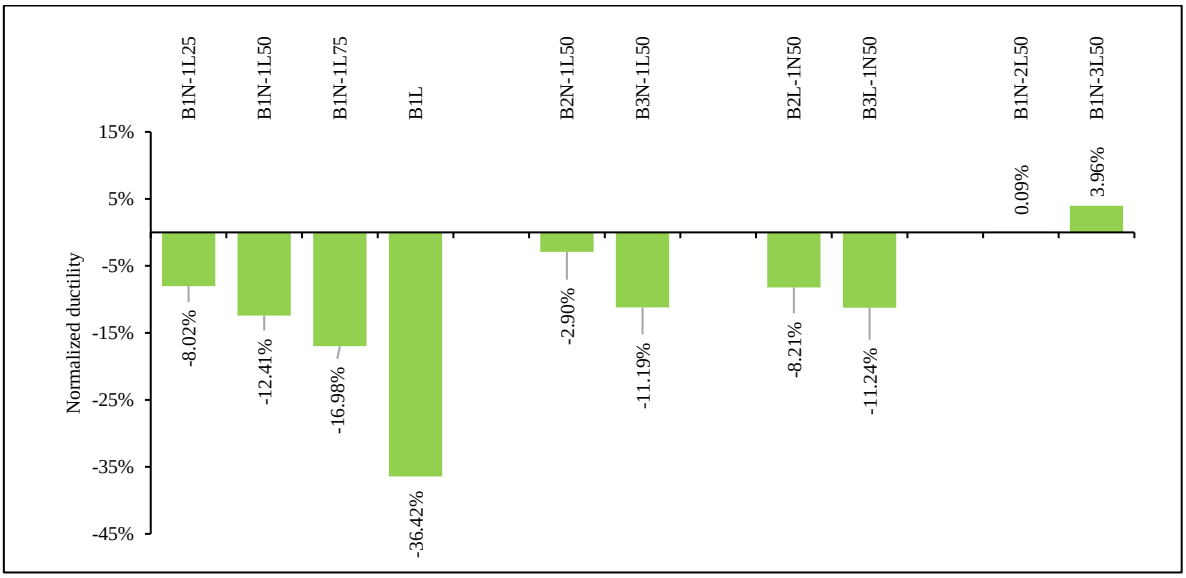

Figure 10. Normalized ductility for the tested beams

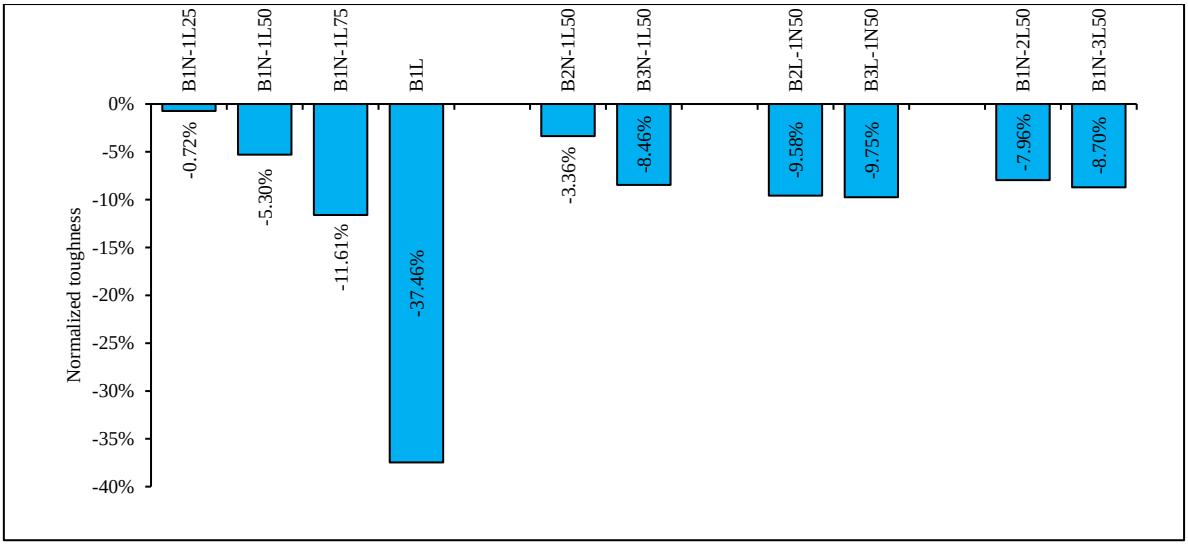

Figure 11. Normalized toughness for the tested beams

5.6. Load-crack opening behavior

Digital crack width meter was used to read the crack opening in the constant moment zone correspond the load manually as shown in Fig.2b. The achieved load-crack width behavior of each beam is presented in Fig. 12. For all the beams in this study were failed with formation of flexural main cracks. The ultimate capacity of these beams was lower than the load required to produce shear cracks due to an intensive amount of shear reinforcement. The results seem to be in agreement with the experimental cracking behavior and failure modes, which indicates that a higher depth ratio resulted in a consistent distribution and lesser crack opening.

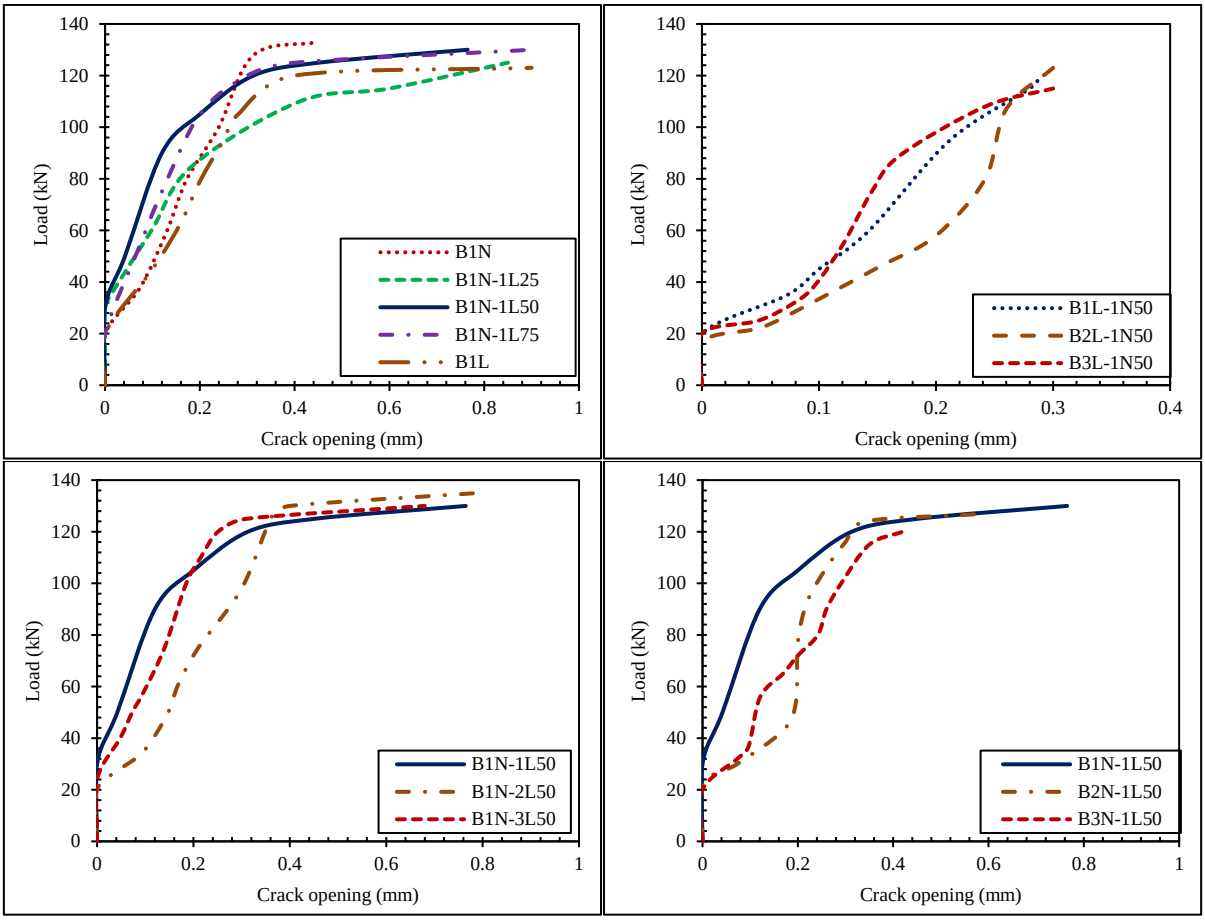

Figure 12. Load-crack opening curves

6. Validation and comparisons

As shown in Figs. 13–15, the experimental results were compared with predicted results using ACI 318-19 Code [14] in terms of cracking moments, service load deflections moment capacities. It is important to point out that there is no availability of papers on constitutive modeling for two-layer beams, which is an interesting subject. The parameters studied and the results presented in this study are unique, and it focus on an area where it has received less attention and is not actually addressed in most design codes.
Theoretical cracking moments of the beams $M_{cr\ (ACI)}$ are determined according to ACI 318-19 Code Eq. 24.2.3.5 [14] as follows:

$$M_{cr(ACI)} = \frac{\lambda f_r I_g}{y_t} \tag{1}$$

Where λ is a reduction factor depends of density of structural lightweight concretes, I_g is the moment of inertia of gross section of concrete beam, y_t represent the distance from extreme fiber of tension to the neutral axis, and f_r modulus of rupture which equal $f_r = 0.62\sqrt{f'_c}$ based on ACI 318-19 Code [14]. These equations are based on beams made with same concrete type for both tension and compression zones. While this study there is two deferent types of concrete these equation needs to be modified as follows:

$$M_{cr(ACI)} = \frac{(\alpha_1 \lambda_1 f_{r1} I_{g1} + \alpha_2\, \lambda_2 f_{r2} I_{g2})}{y_t}. \tag{2}$$

where α_1 represents h_{LW}/h and α_2 is [1-(h_{LW}/h)], while λ_1 and f_{r1} are the reduction factor and modulus of rupture for the first layer, λ_2 and f_{r2} are the reduction factor and modulus of rupture for the second layer. I_{g1} and I_{g2} is the inertia moment for the first and second layers respectively. The experimental and predicted cracking moments are around 80% in agreement, as shown in Fig. 13. This significant level of agreement validates the study's testing procedure and results, indicating that the modified equations can be used.

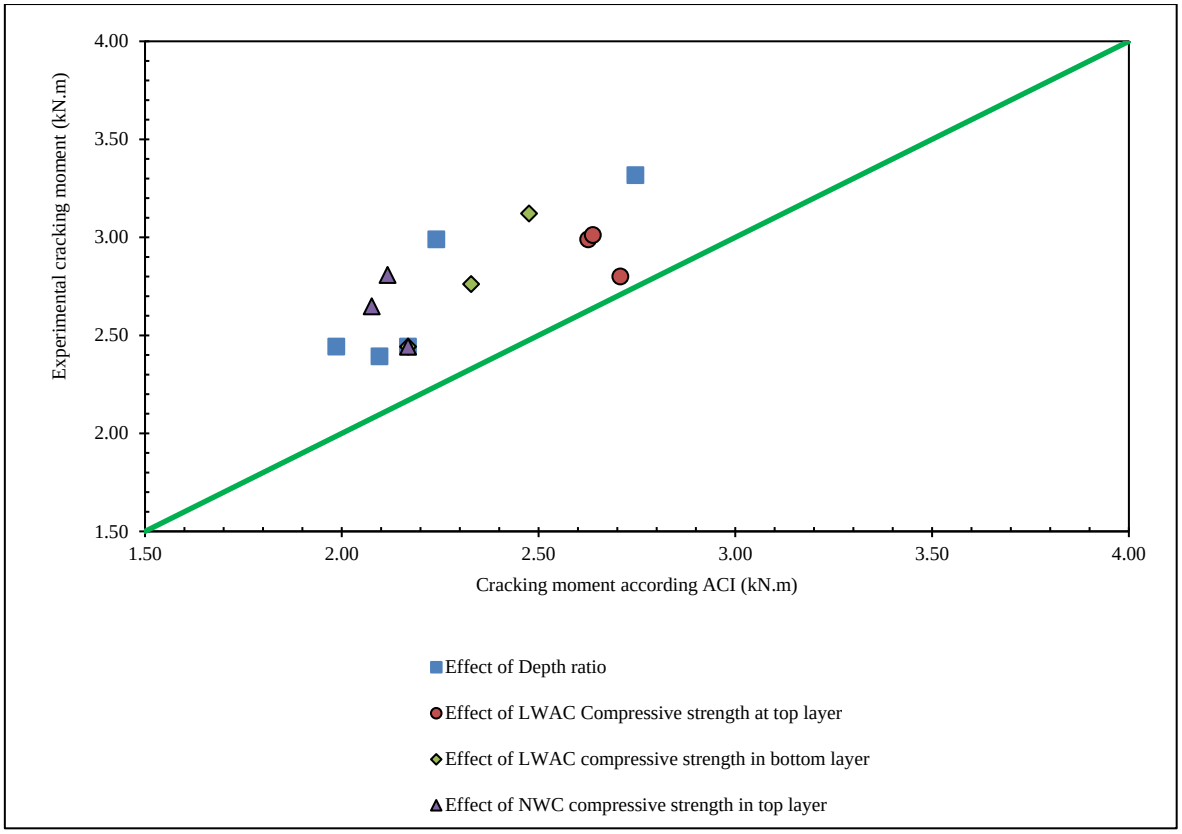

Figure 13. Theoretical versus experimental cracking moments

The experimental and theoretical deflections at service loads are compared in Fig. 14. Using the test setup shown in Fig. 1, the deflection δs of service loads at mid-span is calculated as:

$$\delta_S = \frac{Ma}{24E_cI_e}\left(3L^2 - 4a^2\right) \tag{3}$$

where Ma is the moment at service loads, L is the clear span of beam, a is the projection of distance between load and support, E_c is the modulus of elasticity for concrete as specified in ACI 318-19, $E_c = w_c^{1.5}\, 0.043\sqrt{f_c'}$ and $E_c = 4700\sqrt{f_c'}$ for the lightweight and normal concrete respectively, the effective inertia moment I_e calculated using ACI 318-19 Eq.24.2.3.5a [14] whereas:

$$I_e = \frac{I_{cr}}{1 - \left(1 - \frac{I_g}{I_{cr}}\right)\left(\frac{(2/3)M_{cr}}{M_a}\right)^2} \le I_g \tag{4}$$

$$I_{cr} = \frac{bc^3}{3} + n\,A_s(d-c)^2 + (c-1)A_s'\left(c-d'\right)^2 \tag{5}$$

Where I_{cr} and I_g are the inertia moments for the cracked and gross sections, respectively,

$$n = \frac{E_s}{\alpha_1 E_{c1} + \alpha_2 E_{c2}} \tag{6}$$

The results show an agreement of 86% between the experimental and predicted deflections, which indicates that the modified equations for predicting deflections at service loads are adequate.

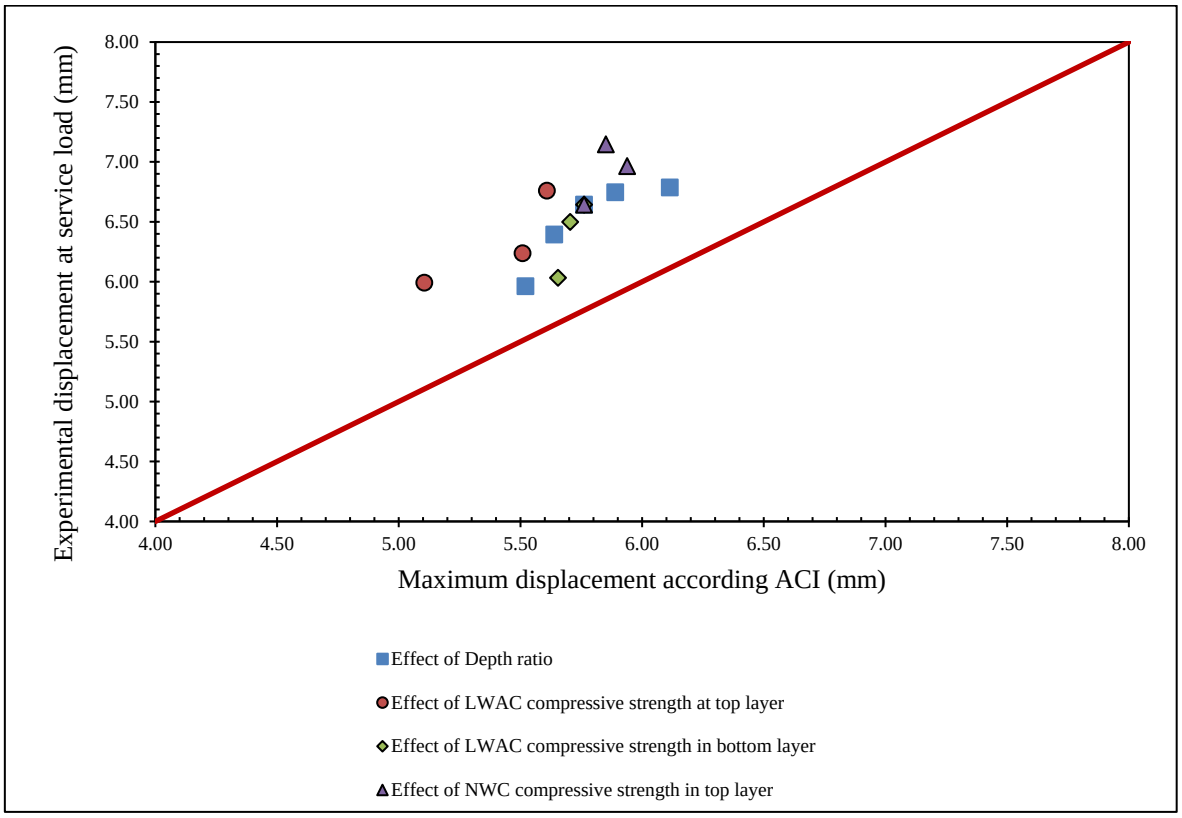

Figure 14. Deflections at service load: experimental vs. theoretical.

The experimental and predicted moment capacities are shown in Fig. 15. Sectional analysis as a doubly reinforced section was used to calculate the nominal moment strength (M_n) as illustrated in Fig. 1. The experimental and theoretical results of moment capacities indicate a good agreement of less than 1% variances. The predicted moments capacity showed that the ACI 318-19 Code handling the structural LWAC beams and two-layer beams similarly as NWC for predicting the cross-section moment capacity of beam is acceptable without modification.

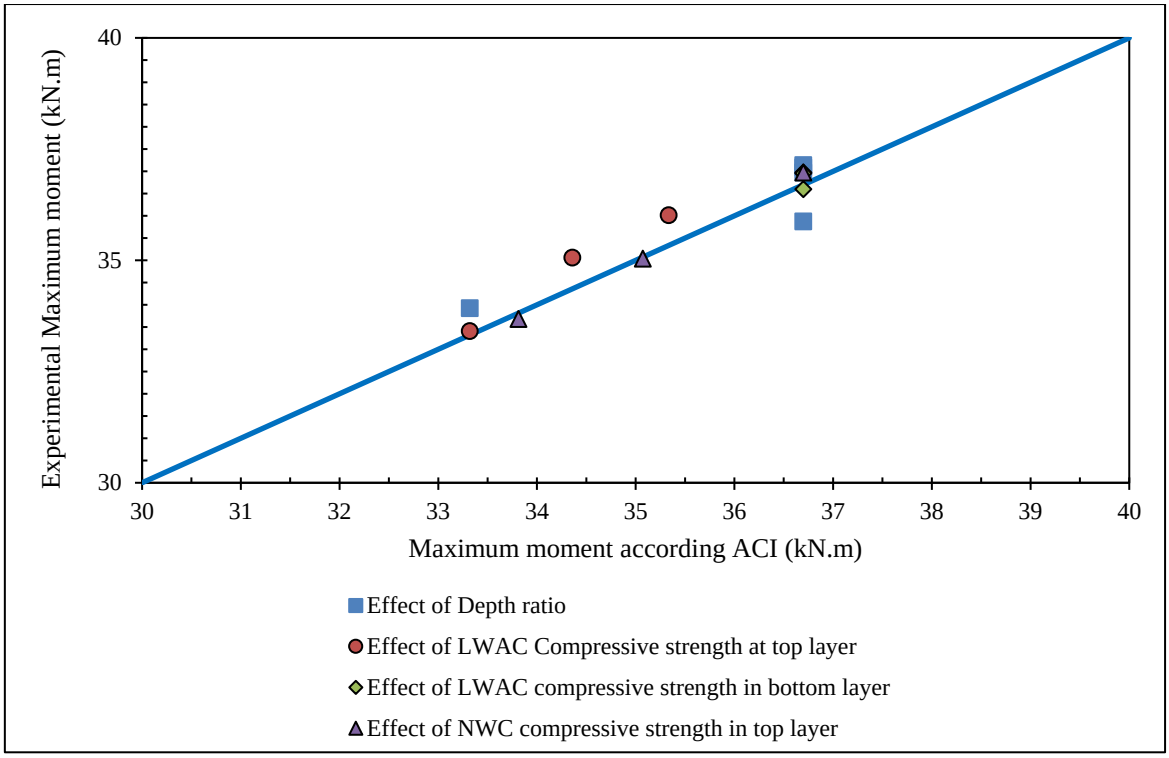

Figure 15. Experimental versus theoretical moment capacity.

7. Conclusions

Based on this study results of this research, the based on the results obtained:

- The behavior of the both control and two-layer beams were similar except for crack spacing, the cracks of two-layer beams were closer to each other in comparison to the cracks of control beams all of the beams failed in flexure.
- Flexural strength: increasing light weight aggregate layer in the tension zone from 0% to 25%, 50%, 75%, and 100% results in an approximately 0.13%, 0.44% ,3.4%, and 8.65% decreases in the ultimate load capacity of beams, respectively.
- Stiffness: The two-layer Beams have no significant changes to each other the initial stiffness, while it is decreased 40% and in compared to beam with full NWC beam and increased 46% in compare to beams with full LWAC beam, while the service stiffness was decreased in average of 4.47% in compared with full NWC beam and increased with an average of 6.68% in compared to LWAC beam. Decreasing the compressive strength of NWC in compression zone decreases the initial and service stiffness. Increasing the LWAC compressive strength in compression zone increases the initial stiffness, while decreases the service stiffness. Increasing the LWAC compressive strength in tension zone increases the initial stiffness while decreases the service stiffness. In all beams, the influence of LWAC layer was more initial stiffness.
- Two layer beams the ductility decreased as hLW/h increased compared to B1N, and increased compared to B1L respectively. Decreasing the compressive strength of NWC and LWAC in compression zone decreases the ductility. In the other hand the ductility increased as the compressive strength of LWAC in tension zone increased.
- The toughness decreased significantly for all beams as compared to control beam of the same group, implying that two-layer beams have a major influence on toughness. The toughness decreased as h_{LW}/h increased compared to B1N, and increased compared to B1L respectively. Decreasing the compressive strength of NWC and LWAC in compression zone the toughness decreased. The toughness decreased as the compressive strength of LWAC in tension zone increased.
- Due to the lack of provisions in the ACI 318-19 Code for predicting the cracking moment, nominal moment capacity, and deflection at service load of two-layer beams, a modification to the equations was proposed. The modified equations demonstrated about 80% agreement with the results of the experimental study.

References

[1] H. K. Adai Al-Farttoosi, O. A. Abdulrazzaq, and H. K. Hussain, "Mechanical Properties of Light Weight Aggregate Concrete Using Pumice as a Coarse Aggregate," *IOP Conf. Ser. Mater. Sci. Eng.*, vol. 1090, no. 1, p. 012106, 2021, doi: 10.1088/1757-899x/1090/1/012106.

[2] G. Campione and L. La Mendola, "Stress-strain behavior in compression of lightweight fiber reinforced concrete under monotonic and cyclic loads," *Adv. Earthq. Eng.*, vol. 9, pp. 387–396, 2001.

[3] F. Altun and T. Haktanir, "Flexural behavior of composite reinforced concrete elements," *J. Mater. Civ. Eng.*, vol. 13, no. 4, pp. 255–259, 2001.

[4] M. A. Adil and O. A. Abdulrazzaq, "Flexural Behavior of Composite Reinforced Concrete Slabs," *Iraqi J. Civ. Eng.*, vol. 11, no. 2, pp. 55–65, 2017.

[5] W. Ferdous, A. Manalo, T. Aravinthan, and A. Fam, "Flexural and shear behaviour of layered sandwich beams," *Constr. Build. Mater.*, vol. 173, pp. 429–442, 2018, doi: 10.1016/j.conbuildmat.2018.04.068.

[6] I. Iskhakov, Y. Ribakov, K. Holschemacher, and T. Mueller, "Experimental investigation of full scale two-layer reinforced concrete beams," *Mech. Adv. Mater. Struct.*, vol. 21, no. 4, pp. 273–283, 2014, doi: 10.1080/15376494.2012.680673.

[7] I. Iskhakov, Y. Ribakov, and K. Holschemacher, "Experimental investigation of continuous two-layer reinforced concrete beams," *Struct. Concr.*, vol. 18, no. 1, pp. 205–215, 2017, doi: 10.1002/suco.201600027.

[8] A. R. Krishnaraja and S. Kandasamy, "Flexural performance of hybrid engineered cementitious composite layered reinforced concrete beams," *Period. Polytech. Civ. Eng.*, vol. 62, no. 4, pp. 921–929, 2018, doi: 10.3311/PPci.11748.

[9] M. Velmurugan, S. Kesavraman, and A. Radhakrishnan, "Experimental study on flexural behaviours of ECC and concrete composite reinforced beams," *Int. J. Civ. Eng. Technol.*, vol. 8, no. 2, pp. 282–288, 2017.

[10] W. J. Ge, A. F. Ashour, X. Ji, C. Cai, and D. F. Cao, "Flexural behavior of ECC-concrete composite beams reinforced with steel bars," *Constr. Build. Mater.*, vol. 159, pp. 175–188, 2018, doi: 10.1016/j.conbuildmat.2017.10.101.

[11] S. J. Mohsin and N. S. Mohammed, "Nonlinear analysis of hybrid reinforced concrete beams under flexural load," *IOP Conf. Ser. Mater. Sci. Eng.*, vol. 737, no. 1, pp. 1–10, 2020, doi: 10.1088/1757-899X/737/1/012022.

[12] P. Dybeł and D. Wałach, "Evaluation of the Development of Bond Strength between Two Concrete Layers," in *IOP Conference Series: Materials Science and Engineering*, 2017, vol. 245, no. 3, doi: 10.1088/1757-899X/245/3/032056.

[13] M. Alhassan, R. Al-Rousan, and A. Ababneh, "Flexural behavior of lightweight concrete beams encompassing various dosages of macro synthetic fibers and steel ratios," *Case Stud. Constr. Mater.*, vol. 7, no. September, pp. 280–293, 2017, doi: 10.1016/j.cscm.2017.09.004.

[14] ACI 318, "318M–19: Building Code Requirements for Reinforced Concrete and Commentary," p. 261, 2019.